DOI: 10.1002/ejic.200900714

Theoretical Analysis of the Possible Intermediates in the Formation of $[W_6O_{19}]^{2-}$

Laia Vilà-Nadal,[a] Antonio Rodríguez-Fortea,*[a] and Josep M. Poblet*[a]

Keywords: Polyoxometalates / Density functional calculations / Molecular dynamics / Solvation methods / Anions

The structural features and the dynamic behaviour of different possible intermediates in the formation of the Lindqvist anion, $[W_6O_{19}]^{2-}$, according to the stoichiometries observed in electrospray fragmentation experiments, were analyzed by DFT calculations. Two different and complementary techniques were used to take into account the effect of the solvent in the computations: (i) continuum solvation models and (ii) Car–Parrinello simulations with explicit solvent molecules. The interaction of the W^{VI} ions with the nucleophilic water molecules expands their coordination sphere, reaching in many cases octahedral coordination. Furthermore, a common structural motif ("building block") is observed in the most stable structures of the intermediates with higher nuclearities.

Introduction

Polyoxometalates (POMs) are an immense class of polynuclear metal–oxygen clusters usually formed by W, Mo or V and mixtures of these elements in their highest oxidation states.[1–4] POMs were first reported in the 19th century,[5] and since then they have been widely studied. The smallest clusters are made up of 6 metal atoms, but much higher nuclearities up to 368 are also found.[6] As a result of their unique physical and chemical properties, POMs have potential applications in many fields, for example, medicine, catalysis, materials science, molecular magnetism, chemical analysis and so on.[1–3] POMs are usually classified into two groups: (i) isopolyanions (IPAs), which are oxides of only one type of M atom, $[M_mO_y]^{q-}$, and (ii) heteropolyanions (HPAs), with the formula $[X_rM_mO_y]^{q-}$, where X is the so-called heteroatom. Both HPAs and IPAs have been prepared and isolated from both aqueous and nonaqueous solutions.[4] The most common synthetic method involves acidification of alkaline aqueous solutions of simple oxido anions and, for HPAs, the necessary heteroatoms. Moreover, control of pH and temperature may be necessary. Formally, it is common to represent the formation of IPAs from mononuclear tungstate anions by Equation (1) from which a theoretical H^+/W ratio on a scale between 0.0 and 2.0 can be assigned (i.e., p/x). All the characterized IPAs show H^+/W ratios higher than 1.[7]

$$x\,[WO_4]^{2-} + p\,H^+ \rightarrow [W_xO_y(OH)_z]^{n-} + (p - z)/2\,H_2O \quad (1)$$

Despite the considerable experimental and theoretical research done during the last decades,[8–14] only few works were devoted to analyzing the formation mechanisms of POMs. Kepert, in the early 1960s, suggested that formation of IPAs might involve the addition of WO_4 tetrahedra. The first step would imply the addition of a WO_4 unit, acting as a bidentate ligand, to a second WO_4 moiety by expanding the coordination number of the latter metal ion to six (Scheme 1).[15] Nucleation is considered to be initiated when the $[WO_4]^{2-}$ anions are protonated, $[WO_3(OH)]^-$, and oneW–O bond is thus stretched in each tetrahedron. After protonation, the W atom becomes more electrophilic and can be more effectively attacked by the O atoms of the $[WO_4]^{2-}$ anion. In the late 1970s, Tytko and Glemser proposed elaborate mechanisms to explain the formation of IPAs and HPAs on the basis of the addition process proposed by Kepert.[16] Besides, they also incorporated in their mechanisms the fact that aggregation of monomers to yield large POMs requires the condensation of H_2O molecules at different reaction steps. There is, however, little experimental evidence to support these mechanisms and some of them do not even agree with experiments.[4]

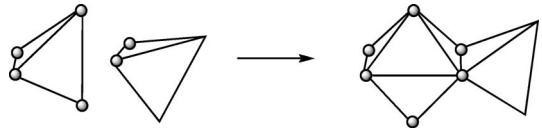

Scheme 1. Addition of two WO_4 tetrahedra as suggested by Kepert.

During the last years, some authors have focused on the initial step of aggregation, that is, the dimerization process.[17] Casey and Rustad performed studies about the rates

[a] Departament de Química Física i Inorgànica, Universitat Rovira i Virgili,
C/Marcel lí Domingo, s/n 43007, Spain
Fax: +34-977-559-569
E-mail: antonio.rodriguezf@urv.cat
josepmaria.poblet@urv.cat

Supporting information for this article is available on the WWW under http://dx.doi.org/10.1002/ejic.200900714.

of oxygen exchange between the $[H_xM_6O_{19}]^{(8-x)-}$ anions (M = Nb, Ta) and aqueous solutions showing the reversibility of M–O bond breaking and formation.[18] Moreover, pathways for oligomerization and dissociation of trivalent metal hydroxide clusters have been proposed.[19] Recently, mechanisms for the nucleation of the Lindqvist anion $[W_6O_{19}]^{2-}$ have been put forward by Cronin and Poblet in a collaborative work that combined theoretical predictions and electrospray ionization mass spectrometry (ESI-MS) experiments.[20] The authors postulated two mechanisms, which were based on successive steps of aggregation of $[WO_3(OH)]^-$ monomers with subsequent protonation and water condensation, to justify the clusters that are observed in the ESI-MS fragmentation experiments, that is, $[WO_3(OH)]^-$, $[W_2O_7]^{2-}$, $[W_2O_6(OH)]^-$, $[W_3O_{10}]^{2-}$, $[W_3O_9(OH)]^-$, $[W_4O_{13}]^{2-}$, $[W_4O_{12}(OH)]^-$, $[W_5O_{16}]^{2-}$, $[W_6O_{19}]^{2-}$ and $[W_6O_{18}(OH)]^-$. We herein analyze in detail different possible structures for each of these stoichiometries by using computational techniques that incorporate the effect of the solvent in two different ways. For dinuclear and trinuclear species, the solvent molecules are considered explicitly by means of Car–Parrinello molecular dynamics (MD) simulations. For larger clusters, the solvent is considered as a continuum model in standard DFT methods. The paper is organized as follows: first, we focus on the results obtained from Car–Parrinello simulations for dinuclear and trinuclear systems, and then second, we present a thorough analysis of possible structural isomers for larger nuclearities.

Results and Discussion

The different isomeric species that can be formed at successive steps of aggregation are analyzed here. We will focus on their relative stability and, in some cases, on the kinetics of their formation. We first analyze dinuclear and trinuclear species in more detail and then we focus on species of higher nuclearity that could lead to the Lindqvist anion.

Dinuclear Clusters

Reaction energies for dinuclear species with respect to two monomers, $[WO_3(OH)]^-$, [Equation (2)] computed at the BP86/COSMO level are listed in Table 1. The structures of the most representative geometries are displayed in Figure 1.

$$2[WO_3(OH)]^- \rightarrow [W_2O_6(OH)_2]^{2-} \quad (2)$$

Table 1. Reaction energies (RE) for dinuclear species with respect to two monomers computed at the BP86/COSMO level.

Stoichiometry	Isomer	RE (kcal mol^{-1})
$[W_2O_6(OH)_2]^{2-}$	**1**	–7.4
	2	+0.3
	3	+10.6
$[W_2O_7]^{2-}$	**1**	–4.4

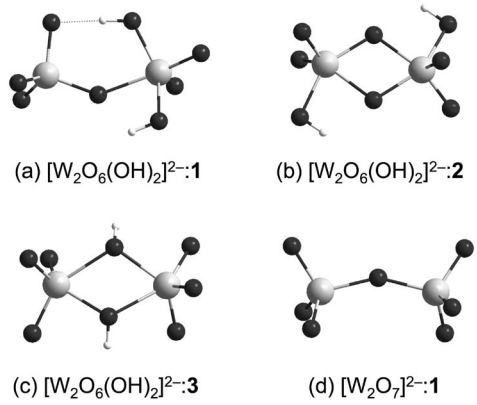

Figure 1. Optimized structures for the most representative dinuclear species.

The lowest-energy minimum, $[W_2O_6(OH)_2]^{2-}$/**1**, found at –7.4 kcal mol^{-1} with respect to the monomers, corresponds to a structure in which one W atom is four-coordinate and the other W atom is five-coordinate (a 5c–4c structure). This structure shows an intramolecular hydrogen bond (Figure 1a). The second most stable dimer (i.e., **2**) is the structure in which the two W atoms are five-coordinate (a 5c–5c structure) and the H atoms are located at the terminal O atoms (Figure 1b). Structure $[W_2O_6(OH)_2]^{2-}$/**2** is around 8 kcal mol^{-1} more unstable than structure **1**. This geometry is not stabilized by intramolecular hydrogen bonds as occurs for structure **1**. When explicit solvent molecules, H_2O in our case, surround the dimer, the O and H atoms of the latter are able to form H bonds with water molecules. Consequently, the strengths of the intramolecular hydrogen bonds are reduced. The way in which the continuous models of solvation take into account this point would be a possible source of error. The quantitative estimation of this error is not straightforward and is out of the scope of this work. Structure $[W_2O_6(OH)_2]^{2-}$/**3** consists of a 5c–5c framework with H atoms at the bridging positions (Figure 1c). It is more than 10 kcal mol^{-1} less stable than structure **2**. The only difference between both structures is the position of the H atoms. Consequently, we can state that for dinuclear species with $[W_2O_6(OH)_2]^{2-}$ stoichiometry, terminal O atoms are more basic than those in the bridging positions in contrast to the behaviour observed for large POMs in which the bridging positions are those with highest basicity.[21] Interestingly, the dinuclear species proposed by Keppert for the first step in the aggregation process, i.e., a 6c–4c structure (Scheme 1), is not located as a minimum in the potential energy surface (PES) when conventional geometry optimization methods are applied. All the geometry optimization attempts starting from a 6c–4c structure lead to 5c–5c structures.

Car–Parrinello MD simulations treating the solvent molecules explicitly at the DFT level were also performed.[22] The metadynamics approach was used to accelerate the dynamics and to compute free-energy barriers.[23–25] The system was formed by 2 $[WO_3(OH)]^-$ monomers and 27 H_2O molecules.[20] Such a computational strat-

egy has been proved to be valid in the study of the hydration of hydrogentungstate anions under different pH conditions.[26] To describe the formation of dinuclear species in solution three collective variables (CV) were used: the coordination number (CN) of each W atom with respect to the eight O atoms that belong to the WO_4 groups, C_{W1-O} and C_{W2-O}; and a conditioned CN, C_{W-O-H}, to account for the number of H atoms bonded to those O atoms bonded to W. The first two CNs explore the phase space related to the formation of dinuclear species and the third CN accounts for the level of protonation/hydration of these species. In Figure 2, the evolution of the coordination numbers C_{W1-O} and C_{W2-O} along the 11-ps metadynamics trajectory is depicted. The first observed event is a H^+ transfer from one $[WO_3(OH)]^-$ monomer to the other, indicating that a H^+ transfer processes between monomers when they are close enough are highly probable. At about 0.6 ps, dimerization takes place to yield a structure in which one W atom is four-coordinate and the other W atom is five-coordinate (a 5c–4c structure, see Figures 1 and 2). Afterwards, the formation of a 5c–5c structure that remains for around 3.5 ps is observed. One interesting structure with a H_2O molecule at the sixth coordination position of one of the W atoms is also seen. Because such a coordination process is not accelerated by metadynamics, water coordination is thought to be a likely process once the dimer is formed. Finally, recrossing to the 5c–4c structure and to the two monomers is observed. The free-energy surface (FES) explored by the metadynamics run can be evaluated directly through the added time-dependent potential. Such a method has been proved to be a reasonable approximation to the free-energy barrier, $\Delta F^{\#}$.[27–34] The free-energy profile shows that the lowest barrier corresponds to the formation of the 5c–4c structure from the two $[WO_3(OH)]^-$ monomers, 7 ± 3 kcal mol^{-1}.[20] From the 5c–4c minimum two processes are equally probable (within the error): the system can escape to the 5c–5c structure or come back to form the monomers. All these barriers can be easily overcome at temperatures that are necessary to form IPAs (ambient temperature or even higher). The 5c–4c structure is around 9 ± 3 kcal mol^{-1} more stable than the system formed by the two monomers. The 5c–5c structure is almost degenerate with the 5c–4c structure. It is worth noting here that the 6c–4c structure proposed by Kepert is not observed during the metadynamics. Thus, this type of dimer, if it exists, must have a higher barrier of formation than the 5c–4c and 5c–5c structures.

Additional metadynamics runs with the use of other sets of collective variables (CV) were also performed, and the main features of the previous simulation were retrieved.[20] During the metadynamics simulations, dinuclear species appear hydrated for rather long periods of time. To examine the relative stability of such structures, we took several snapshots from our simulations that cover a wide range of coordination situations, and we optimized them in a dynamical way. We performed dynamic optimization of the structure by reducing progressively the temperature of the system (annealing) up to a very low value (1 K in our case).

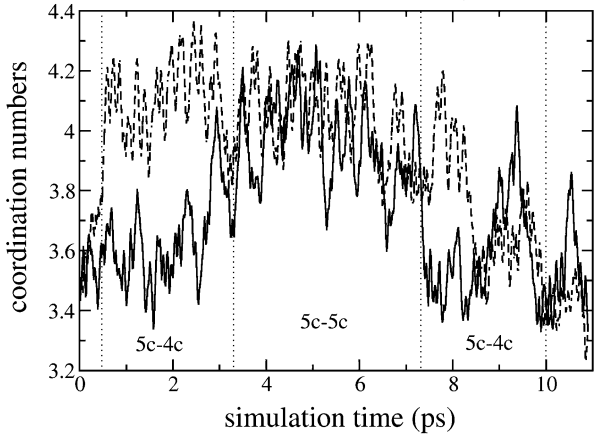

Figure 2. Evolution of the coordination numbers C_{W1-O} and C_{W2-O} along the trajectory of the metadynamics run. Vertical dotted lines separate the regions where different structures appear.

We have to be aware that these calculations provide us with the energy of the whole system, that is, the tungstate dimer and the water molecules in the simulation box. Therefore, a particularly stable configuration of water molecules may counterbalance a not so favourable dimer structure. To escape this possible source of error, we only focussed on the general trends observed in these optimizations. The results (Table S1, Supporting Information) show that monohydrated 5c–5c structures (Figure S1, Supporting Information) are in general more stable than nonhydrated 5c–5c and monohydrated 5c–4c dimers.

The effect of the pH in the formation of dinuclear species was also analyzed by simulations under low pH conditions with two $WO_2(OH)_2$ monomers surrounded by 27 H_2O molecules.[20] Formation of a hydrated 5c–4c structure is already observed in a standard Car–Parrinello MD. Therefore, a low energy barrier for the dimerization process can be inferred. Formation of dinuclear species under low pH conditions is found to be favoured from metadynamics simulations. Moreover, dehydration of the 5c–4c structure is much more feasible than under medium pH conditions.[20] The 6c–4c structure proposed by Kepert is not observed under these conditions. Similarly to the case of medium pH conditions, annealings for some representative dinuclear species have been performed. The results (Table S2, Supporting Information) show that hydration gives extra stability to dimers and that the lowest-energy species show hexacoordinate W^{VI} ions (Figure 3). The larger the number of protons bonded to the dinuclear structure, that is, the electrophilic character of W^{VI} ions, the larger the stabilization after coordination of nucleophilic water molecules.

Once the aggregation of two $[WO_3(OH)]^-$ monomers takes place, a long way still remains before arriving at the Lindqvist anion $[W_6O_{19}]^{2-}$. Two formation mechanisms, based on consecutive steps of nucleation and water condensation, are proposed that are consistent with the ESI-MS experiments.[20] For each of the stoichiometries, $[W_3O_{10}]^{2-}$, $[W_3O_9(OH)]^-$, $[W_4O_{13}]^{2-}$, $[W_4O_{12}(OH)]^-$, $[W_5O_{16}]^{2-}$, $[W_6O_{19}]^{2-}$ and $[W_6O_{18}(OH)]^-$, a search for the lowest-energy

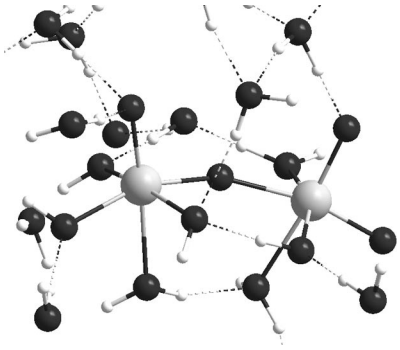

Figure 3. Optimized structure for the most stable dinuclear species in solution under low pH conditions, 5c+1w–4c+2w (w stands for coordinated H_2O). The two W atoms are hexacoordinate.

structure was performed. The structures with four or more W atoms were only computed at the BP86/COSMO level, because the explicit inclusion of water molecules to perform Car–Parrinello simulations is prohibitively expensive from a computational point of view.

Trinuclear Clusters

Relative energies and geometries for representative trinuclear species with stoichiometries according to the proposed mechanism M1 by Poblet and Cronin, $[W_3O_{10}(OH)]^{3-}$ and $[W_3O_{10}]^{2-}$, are presented here (see Supporting Information for a description of the mechanisms).[20] The structures corresponding to stoichiometries derived from mechanism M2 are almost identical to those of M1 with an extra H atom. This H atom can be attached in many different positions, and the most stable position corresponding to the most basic O atom. Because analysis of the basicity of the different O atoms for all of these intermediate structures is out of the scope of the present work, this question will not be discussed here. Both compact structures, $[W_3O_{10}(OH)]^{3-}$ and $[W_3O_{10}]^{2-}$, have a tricoordinated μ_3-O atom (Figure 4). For $[W_3O_{10}(OH)]^{3-}$, the W_3O_3 central core (three W, two μ_2-O and the μ_3-O ligand) is planar.

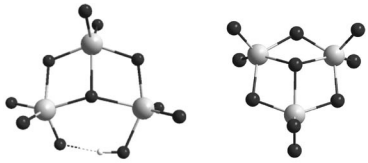

Figure 4. Optimized structures for the most representative trinuclear species.

The structure of $[W_3O_{10}(OH)]^{3-}$ shown here is computed to be more stable (at least by 8 kcal mol^{-1}) than other more open isomers with μ_2-O atoms (see Table S3 and Figure S2, Supporting Information). Interestingly, the structure of $[W_3O_{10}]^{2-}$ is identical to that recently found by Müller and co-workers for a trinuclear cluster in the cavity of a Mo/W storage protein.[35] This unit is also present as a constituent of the well-known $[W_{12}O_{40}H_2]^{6-}$ species.[36] It is also remarkable that the planar W_3 structural motifs must confer high stability to the structure because they are also found in clusters with higher nuclearities (vide infra). Thus, these planar W_3 motifs can be considered as structural *building blocks*. The formation and the stability of trinuclear clusters under acidic conditions were also analyzed by Car–Parrinello metadynamics, even though these simulations have an important computational cost. The system consists of one dimer $[W_2O_7]^{2-}$, one monomer $[WO_3(OH)]^-$, 57 H_2O and two H_3O^+. In this metadynamics run, we are more interested in visiting efficiently the phase space than in estimating the free-energy barriers. Two CVs were chosen: a CN of the W atoms of the dimer with respect to the O atoms of the WO_4 groups, C_{Wdim-O}, and a conditioned CN that counts for the number of W–O–W bonds formed by the W atom in the monomer with the W atoms in the dimer (see Computational Methodology). Open trimers are formed firstly. Furthermore, we observe that closed and not very tensioned trinuclear clusters are more stable than open structures (see Table S4, Supporting Information). Two low-energy structures were found to feature a threefold coordinated O atom (μ_3-O), but a closed cluster with only twofold coordinated O atoms (μ_2-O) is also very stable (Figure 5). The structure shown in Figure 5c is analogous to the lowest-energy structure found by using the COSMO methodology to simulate the solvent (Figure 4, left).

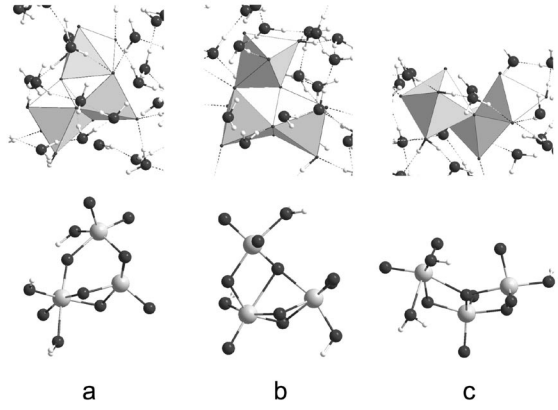

Figure 5. Polyhedral (top) representation for the optimized structures of some characteristic trinuclear species $[W_3O_9(OH)_2]^{2-}$ in solution: (a) μ_2-O 5c+1w–5c–5c structure; (b) μ_3-O 6c–6c–4c+1w structure; (c) μ_3-O 5c+1w–5c–5c structure. Ball-and-stick representations without the surrounding water molecules are also displayed (bottom).

In order to analyze the stability of $[W_3O_{10}]^{2-}$ in water, we performed a standard Car–Parrinello molecular dynamics run for the system formed by $[W_3O_{10}]^{2-}$ and 58 H_2O molecules. After approximately 5 ps of equilibration, a molecular dynamics of 20 ps was done. During the equilibration, a water molecule was already coordinated to one of the W ions (W1), occupying its sixth coordination position and yielding an octahedral environment around it. After this process of coordination, the structure of the cluster was preserved. We will briefly describe here the most interesting events observed during the 20 ps dynamics. At the beginning, hydrolysis of the water ligand, that is, formation of

$[W_3O_{10}(OH)]^{3-}$ species, was observed. The released proton was transferred by two solvent molecules to an oxido ligand of the cluster, that is, an intramolecular proton transfer mediated by the solvent molecules occurred. So, at 3 ps the initial $[W_3O_{10}(H_2O)]^{2-}$ cluster had become $[W_3O_9(OH)_2]^{2-}$, with one W ion (W1) having four oxido and two hydroxido ligands and the other two keeping their original five oxido ligands (see Figure 6).

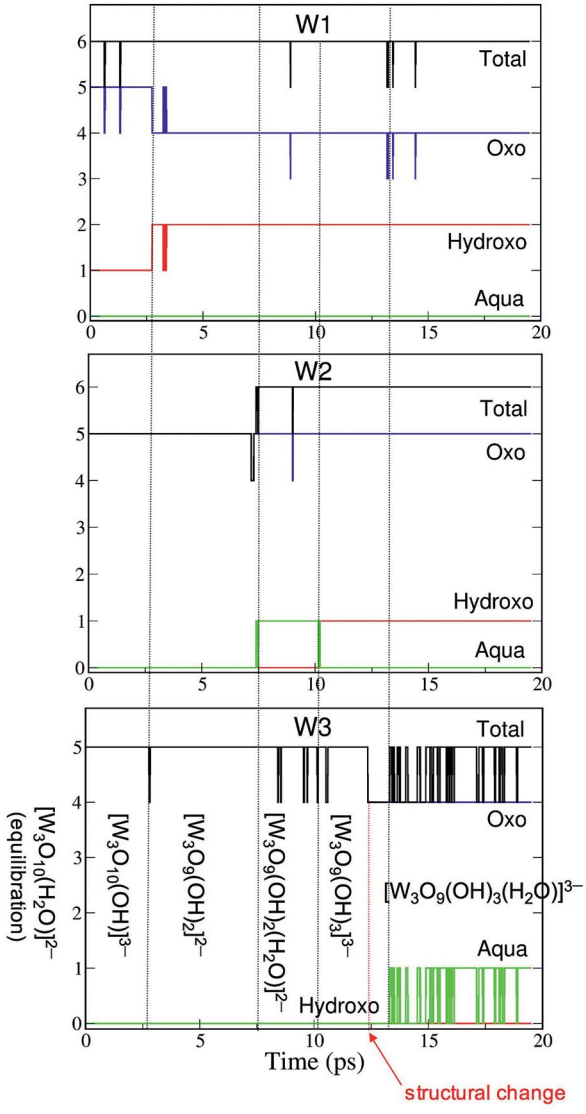

Figure 6. Number of oxido, hydroxido and aqua ligands as well as the total number of ligands for each of the W ions during the molecular dynamics simulation of $[W_3O_{10}]^{2-}$ and 58 H_2O molecules (W1, top; W2, middle; W3, bottom). The coordination numbers of W1 and W3 are six and five, respectively, during almost all of the simulation; W2, however, shows coordination five at the beginning (up to 7.5 ps) and coordination six afterwards. The species at each time interval are shown in the bottom plot.

The structure of $[W_3O_9(OH)_2]^{2-}$ is then kept for 4 ps, and the water molecules interact with the O and H atoms of the cluster through hydrogen bonds. At around 7.5 ps, coordination of a water molecule to one of the remaining five-coordinate W ions (W2) is observed. The cluster $[W_3O_9(OH)_2(H_2O)]^{2-}$, now with two six- and one five-coordinate W ions, preserves its original structure. At around 10 ps, the water molecule that is coordinated to one of the W ions (W2) is hydrolyzed, that is, a proton is released to the solution to form a hydronium cation and a cluster of the type $[W_3O_9(OH)_3]^{3-}$. At 12.5 ps, the structure of the cluster undergoes a significant change: the bond between the five-coordinate W ion (W3) and the μ_3-O ligand is broken, leading to a μ_2-O ligand and a four-coordinate W ion (Figure 6, bottom). The new W_3 framework is very similar to the structure shown in Figure 5a. Only 1 ps later, another water molecule is attached to the four-coordinate W ion (W3), forming a cluster with stoichiometry $[W_3O_9(OH)_3(H_2O)]^{3-}$. This cluster, with two six- and one five-coordinate W ions keeps its structure up to the end of the simulation.

Figure 7 displays the W–O radial distribution function of one of the W ions that constitute the cluster, W1, along with its integration that yields the coordination number of W1 during the simulation. The sharp spike below 2 Å that integrates to one O atom can be attributed to the terminal oxido ligands. The spike with a maximum around 2 Å, and which is extended up to 2.5 Å, integrates to five O atoms. Two of these five O atoms correspond to hydroxido ligands (with bonds around 2 Å) and the other three O atoms are attributed to bridging oxido ligands, which feature longer W–O bond lengths. At distances between 2.5 and 3.5 Å, the W1–O coordination number shows a plateau associated with the presence of six O atoms in the coordination sphere of the W1 ion. A shallow maximum appears at distances between 4 and 5 Å, which is associated to the first solvation sphere and to the rest of the O atoms that belong to the cluster; most of them are found at distances between 4 and 5 Å. The W–O radial distribution functions for W2 and W3 are displayed in the Supporting Information (Figure S3).

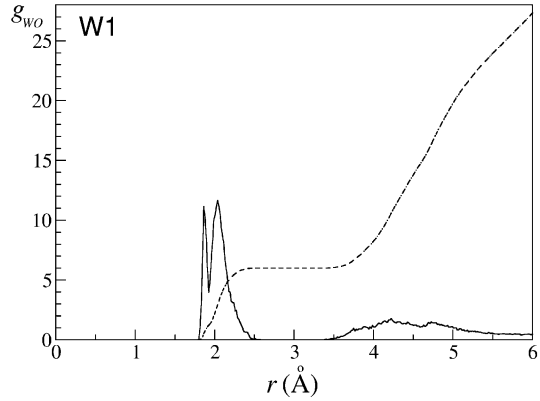

Figure 7. W–O radial distribution function, $g_{WO}(r)$ (solid line) and its integration, the coordination number (broken line) of W1 for 20 ps of MD simulation starting from $[W_3O_{10}(H_2O)]^{2-}$.

From the present simulation we can conclude that the W^{VI} ions in the trinuclear $[W_3O_{10}]^{2-}$ cluster coordinate water molecules to have octahedral coordination spheres. These water molecules undergo hydrolysis processes to yield hydroxido ligands through intramolecular proton transfers or by releasing protons to the solution. So, in the presence

of hydrogentungstate monomers, the nucleophilic O atoms of these anions coordinate to W^{VI} ions of the trinuclear cluster to saturate their coordination spheres, yielding the tetranuclear species.

From Tetranuclear Species to the Lindqvist Anion

Relative energies for $[W_4O_{13}]^{2-}$, $[W_4O_{13}(OH)]^{3-}$, $[W_5O_{16}]^{2-}$ and $[W_5O_{16}(OH)]^{3-}$ species with respect to their most stable isomer are listed in Table 2. Their geometries are displayed in Figures 8 and 9. The most stable structure that we found for a $[W_4O_{13}]^{2-}$ stoichiometry, **1**, corresponds to a compact cluster with a fourfold coordinated O atom (μ_4-O). This structure is 7.6 kcal mol^{-1} more stable than $[W_4O_{13}]^{2-}$:**2**. So, we infer that the planar conformation of structure **1** and the μ_4-O atom confers an extra stability to tetranuclear clusters. In the case of $[W_4O_{13}(OH)]^{3-}$, the most stable structure (i.e., **1**) is again a planar tetramer. This structure can also be seen as a trinuclear planar motif with an extra W atom attached to two W atoms belonging to the trimer. In comparison to $[W_4O_{13}(OH)]^{3-}$/**3**, the extra W atom of structure **1** is attached to two oxygen atoms, this fact contributing to a major stabilization of the structure. Although structure **4** is more compact than the others, it appears to be less stable. This could be explained due to the loss of planarity of the W_3 motifs within this structure.

Table 2. Relative energies (kcal mol^{-1}) for some representative $[W_xO_y(OH)_z]^{k-}$ tetra- (x = 4, y = 13, z = 0 or 1) and pentanuclear (x = 5, y = 16, z = 0 or 1) species.

Stoichiometry	Isomer	O coordination[a]	ΔE
$[W_4O_{13}]^{2-}$	**1**	4	0.0
	2	2	7.6
$[W_4O_{13}(OH)]^{3-}$	**1**	3	0.0
	2	2	0.2
	3	3	2.7
	4	3	4.6
$[W_5O_{16}]^{2-}$	**1**	3	0.0
	2	5	3.2
	3	3	3.3
$[W_5O_{16}(OH)]^{3-}$	**1**	3	0.0
	2	3	5.7
	3	4	6.1

[a] Highest coordination of an O atom within the cluster.

Regarding the $[W_5O_{16}]^{2-}$ stoichiometry, three structures are found to be the most stable ones, two of them (i.e., **2** and **3**) are quasidegenerate and somewhat more unstable than **1**. Structure **1** features two μ_3-O atoms, each of them within a planar W_3 unit as in the tetranuclear cluster. These planar trinuclear motifs, also present in the Lindqvist anion and in the tetranuclear form, confer stability to the cluster. Structure **2**, which is only 3 kcal mol^{-1} more unstable than **1** and with a μ_5-O atom, shows a framework that fairly resembles that of the Lindqvist anion (see Figures 9 and 10). Although structure **1** is slight more stable than structure **2**, the topology of the latter seems more favourable to lead to the hexametalate. For $[W_5O_{16}(OH)]^{3-}$, again three structures are reported as the most representative ones. The

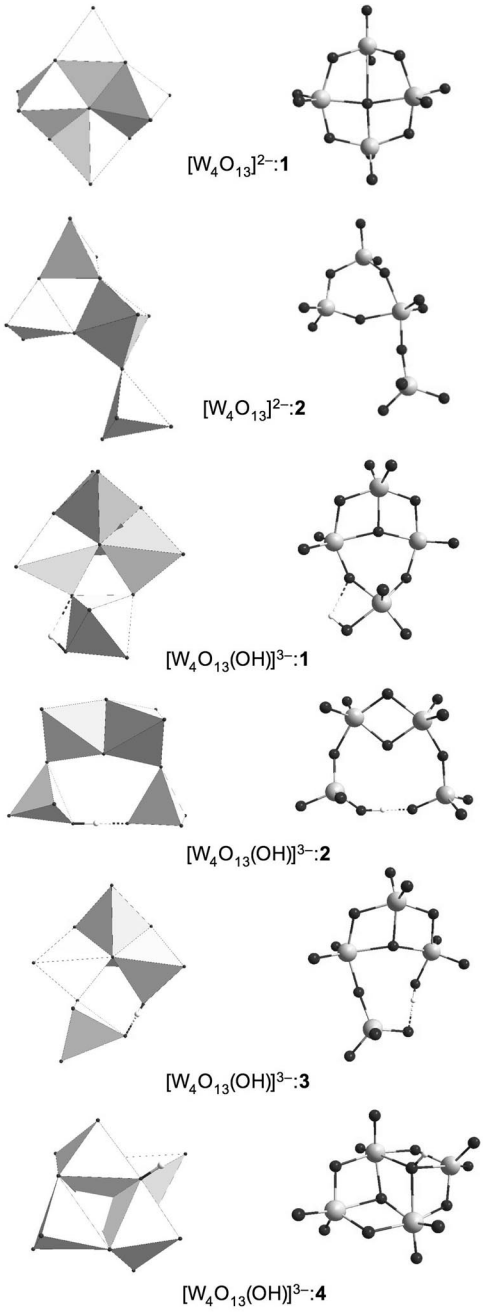

Figure 8. Polyhedral (left) and ball-and-stick (right) representations for the optimized structures of the most representative tetranuclear species. For $[W_4O_{13}]^{2-}$ stoichiometry: structures **1** and **2**; for $[W_4O_{13}(OH)]^{3-}$ stoichiometry: structures **1**, **2**, **3** and **4**.

planar motif W_3 is found in the three structures. Isomer **3** is the less stable despite the presence of a μ_4-O atom probably due to its more tensioned framework.

Finally, the same analysis was performed for hexanuclear species (see Table S5 and Figure S4, Supporting Information). Structures that are far from the Lindqvist anion show higher energies than those that are more similar to it. In Figure 10 one can observe an example of a hexanuclear $[W_6O_{19}(OH)]^{3-}$ structure before evolving towards the Lindqvist anion $[W_6O_{19}]^{2-}$.

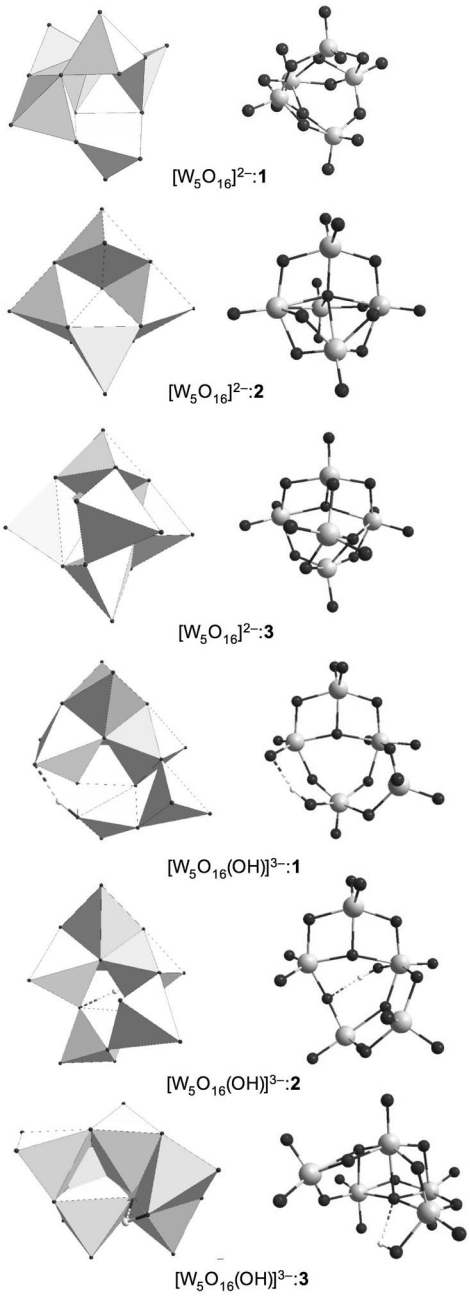

Figure 9. Polyhedral (left) and ball-and-stick (right) representations for the optimized structures of the most representative pentanuclear species. For $[W_5O_{16}]^{2-}$ stoichiometry: structures **1**, **2** and **3**; for $[W_5O_{16}(OH)]^{3-}$ stoichiometry: structures **1**, **2** and **3**.

Conclusions

By making use of two complementary methodologies, that is, (i) standard DFT methods with inclusion of the solvent as a continuum by means of the COSMO model and (ii) Car–Parrinello MD simulations with explicit solvent molecules, we analyzed the structure and the relative energies of different possible intermediates in the formation of the Lindqvist anion $[W_6O_{19}]^{2-}$. Car–Parrinello simulations show that the coordination sphere of the W^{VI} ions might be expanded due to bonding with water molecules. This effect is more important at low pH conditions. Concerning trinuclear species, linear or open structures are more easily formed than compact clusters, but they are not as stable as the latter. Similarly to dinuclear species, coordination of W^{VI} ions is expanded because of the interaction with water molecules. As far as the structural aspects are concerned, a planar W_3 unit is found to be very stable. These W_3 units, which are also observed in clusters with higher nuclearity and even in the Lindqvist anion, act as structural building blocks conferring high stability to the intermediate clusters. Finally, those penta- and hexanuclear clusters that most resemble the Lindqvist anion are within the most stable intermediates. In summary, the complementarity of the structural analysis and the dynamical simulations of the intermediates observed in the ESI-MS experiments provide new insights into the aggregation mechanisms of polyoxometalates with low nuclearities. However, further analogous experimental and theoretical work on other iso- and heteropolyanions is needed to fully accomplish the ambitious purpose of understanding such nucleation mechanisms.

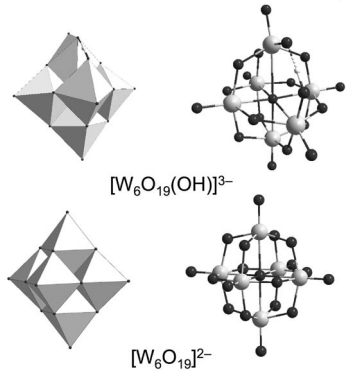

Figure 10. Polyhedral (left) and ball-and-stick (right) representations for the optimized structures corresponding to stoichiometry $[W_6O_{19}(OH)]^{3-}$ and the Lindqvist anion $[W_6O_{19}]^{2-}$.

Computational Methodology

The static calculations were carried out by using density functional theory (DFT) methodology with the ADF 2004 program.[37,38] The gradient-corrected functionals of Becke[39] and Perdew[40] for the exchange and correlation energies, respectively, were used to improve the description of the electronic density provided by the local density approximation (X-alpha functional for the exchange part and Vosko-Wilk-Nusair functional for the correlation part).[41] A set of Slater-type basis functions of triple-ζ + polarization quality was employed to describe the valence electrons of all the atoms. Scalar relativistic corrections were included by the zeroth-order regular approximation (ZORA) formalism. All the computed stationary points have closed-shell electronic structure. All the structures discussed through this work were fully optimized in the presence of a continuous model solvent by the conductor-like screening model (COSMO)[42–44] implemented in the ADF code.[45] To define the cavity that surrounds the molecules we use the solvent accessible surface (SAS) method and a fine tesserae. Once the geometry has been optimized using the SAS surface, we perform single-point calculations by using the solvent excluding surface (SES) that yields more meaningful values for the hydration energies. Geometry opti-

mization using the SES yields "unrealistic" distorted structures when the coordination number of W^{VI} ions is lower than six. To obtain the electron density in solution, first it is converged in the gas phase and afterward the COSMO model is turned on to include the solvent effects variationally. The ionic radii of the atoms, which define the dimensions of the cavity surrounding the molecule, are chosen to be 1.26 for W, 1.52 for O and 1.20 Å for H. The dielectric constant (ε) is set to 78 so as to model water as solvent.

Regarding to the molecular dynamics (MD) simulations, they were performed at the DFT level by means of the CPMD program package.[46] The description of the electronic structure is based on the expansion of the valence electronic wave functions into a plane wave (PW) basis set, which is limited by an energy cutoff of 70 Ry. The interaction between the valence electrons and the ionic cores is treated through the pseudopotential (PP) approximation. Norm-conserving Martins-Troullier PPs are employed.[47] Nonlinear core corrections (NLCC) are included in the W PP.[48] We adopt the generalized gradient-corrected Becke-Lee–Yang–Parr (BLYP) exchange-correlation functional.[39,49] The validity of these computational settings for the study of the hydrogentungstate anion has been checked previously.[26] In the MD simulations, the wave functions are propagated in the Car-Parrinello Scheme, by integrating the equations of motion derived from the extended Car-Parrinello Lagrangian.[22] We use a time step of 0.144 fs and a fictitious electronic mass of 700 au. A simple rescaling of the atomic velocities keeps the temperature within an interval of 50° around 300 K. The cell box that contains: (i) two $[WO_3(OH)]^-$ and 27 H_2O molecules ($a = b = c = 9.959$ Å) or (ii) three $[WO_3(OH)]^-$ and 58 H_2O molecules ($a = b = c = 12.580$ Å) is repeated periodically in space by the standard periodic boundary conditions.

The limited simulation time affordable by standard MD runs does not allow the observation of rare events like thermally activated chemical reactions. For this reason, we employ the metadynamics technique, which is capable of efficiently reconstructing complex reaction mechanisms and provides the free-energy profile, as demonstrated in previous applications.[27–34] A detailed description of the metadynamics method associated with Car–Parrinello MD can be found elsewhere.[23] The metadynamics simulations are based on the selection of collective variables (CV) that are suitable to describe the process. In this work, we often use as CV the coordination number (CN) of one atom, or group of atoms, A, with respect to a second atom, or group of atoms, B.[23,50] The CN provides information on the interaction pattern characterizing the actual atomic configuration. Because it is more general and flexible than other order parameters like bond lengths and bond angles, the risk of biasing the reaction on a predetermined path is largely reduced. The analytic definition of the CN of B with respect to A can be found elsewhere.[23] In the present work, $p = 8$ and $q = 14$ are used. With this definition, we express the CN as a differentiable curve. As a consequence, the CN of one atom with respect to another is not an integer value (in the present case, around 3.5 when the W ions are four-coordinated and around 4 when they are five-coordinate). The parameters used in the metadynamics for the trinuclear system ($[W_2O_7]^{2-}$, $[WO_3(OH)]^-$, 57 H_2O and two H_3O^+) are the following: $k_1 = k_2 = 1.5$ au, $M_1 = M_2 = 20.0$ amu. The height of the hills (W) is 0.75 kcal mol^{-1}, their perpendicular width ($\Delta s^{\perp}$) 0.065 (CV1) and 0.098 (CV2), and the deposition rate (Δt) 0.0108 ps. The total simulation time (t_{total}) was 25 ps.

Supporting Information (see footnote on the first page of this article): Tables showing the relative energies for different dinuclear species obtained from annealing the structures observed in the metadynamics under different pH conditions along with a figure displaying the most stable dinuclear structure at medium pH; table with the relative energies of some representative $[W_3O_9(OH)]^{2-}$ structures along with a picture of their optimized geometries; table with the relative energies for different trinuclear species as obtained from the annealing of structures observed in the metadynamics at low pH conditions; figure depicting the W–O radial distribution function and its integration for W2 and W3 atoms during the 20 ps of MD simulation starting from $[W_3O_{10}(H_2O)]^{2-}$; table with the relative energies of some representative $[W_6O_{19}(OH)]^{3-}$ structures along with a picture showing their optimized geometries; table with the mechanisms for the formation of the Lindqvist anion, $[W_6O_{19}]^{2-}$, as proposed by Poblet and Cronin; optimized coordinates (*xyz* files) for the most representative structures of this work.

Acknowledgments

We acknowledge support from the Ministerio de Educacion (MEC) of Spain (project CTQ2008-06549-C02-01/BQU) and the Ramón y Cajal Program (A.R.F) and from the DGR of the Autonomous Government of Catalonia (grants 2009SGR462 and XRQTC). The authors also acknowledge the computer resources, technical expertise and assistance provided by the Barcelona Supercomputing Center-Centro Nacional de Supercomputación (part of the calculations were performed there).

[1] J. J. Borrás-Almenar, E. Coronado, A. Müller, M. T. Pope, *Polyoxometalate Molecular Science*, Kluwer Academic, Dordrecht, The Netherlands, **2003**.
[2] Special issue on polyoxometalates: C. L. Hill (Guest Editor), *Chem. Rev.* **1998**, *98*, issue 1.
[3] D. L. Long, E. Burkholder, L. Cronin, *Chem. Soc. Rev.* **2007**, *36*, 105–121.
[4] M. T. Pope, *Heteropoly and Isopoly Oxometalates*, Springer, Berlin, **1983**.
[5] J. J. Berzelius, *Ann. Phys. Chem.* **1826**, *6*, 369.
[6] A. Muller, E. Beckmann, H. Bogge, M. Schmidtmann, A. Dress, *Angew. Chem. Int. Ed.* **2002**, *41*, 1162.
[7] R. J. Errington, C. Lax, D. G. Richards, W. Clegg, K. A. Fraser in *Polyoxometalates: From Platonic Solids to Anti-Retroviral Activity*, Kluwer Academic, Dordrecht, The Netherlands, **1994**, pp. 105–114.
[8] A. Bagno, M. Bonchio, *Angew. Chem. Int. Ed.* **2005**, *44*, 2023–2026.
[9] H. Duclusaud, S. A. Borshch, *J. Am. Chem. Soc.* **2001**, *123*, 2825–2829.
[10] J. A. Fernandez, X. Lopez, C. Bo, C. de Graaf, E. J. Baerends, J. M. Poblet, *J. Am. Chem. Soc.* **2007**, *129*, 12244–12253.
[11] D. Kumar, E. Derat, A. M. Khenkin, R. Neumann, S. Shaik, *J. Am. Chem. Soc.* **2005**, *127*, 17712–17718.
[12] J. M. Poblet, X. Lopez, C. Bo, *Chem. Soc. Rev.* **2003**, *32*, 297–308.
[13] D. Quinonero, Y. Wang, K. Morokuma, L. A. Khavrutskii, B. Botar, Y. V. Geletii, C. L. Hill, D. G. Musaev, *J. Phys. Chem. B* **2006**, *110*, 170–173.
[14] L. K. Yan, X. Lopez, J. J. Carbo, R. Sniatynsky, D. C. Duncan, J. M. Poblet, *J. Am. Chem. Soc.* **2008**, *130*, 8223–8233.
[15] D. L. Kepert, *Prog. Inorg. Chem.* **1962**, *4*, 199.
[16] K. H. Tytko, O. Glemser, *Adv. Inorg. Chem. Radiochem.* **1976**, *19*, 239.
[17] S. Messaoudi, E. Furet, R. Gautier, E. Le Fur, J. Y. Pivan, *Phys. Chem. Chem. Phys.* **2004**, *6*, 2083–2087.
[18] E. Balogh, T. M. Anderson, J. R. Rustad, M. Nyman, W. H. Casey, *Inorg. Chem.* **2007**, *46*, 7032–7039.
[19] W. H. Casey, J. R. Rustad, L. Spiccia, *Chem. Eur. J.* **2009**, *15*, 4496–4515.

[20] L. Vila-Nadal, A. Rodriguez-Fortea, L.-K. Yan, E. L. Wilson, L. Cronin, J. M. Poblet, *Angew. Chem. Int. Ed.* **2009**, *48*, 5452–5456.
[21] J. A. Fernandez, X. Lopez, J. M. Poblet, *J. Mol. Catal. A* **2007**, *262*, 236–242.
[22] R. Car, M. Parrinello, *Phys. Rev. Lett.* **1985**, *55*, 2471.
[23] M. Iannuzzi, A. Laio, M. Parrinello, *Phys. Rev. Lett.* **2003**, *90*, 238302.
[24] A. Laio, M. Parrinello, *Proc. Natl. Acad. Sci. USA* **2002**, *99*, 12562.
[25] A. Laio, A. Rodriguez-Fortea, F. L. Gervasio, M. Ceccarelli, M. Parrinello, *J. Phys. Chem. B* **2005**, *109*, 6714–6721.
[26] A. Rodriguez-Fortea, L. Vila-Nadal, J. M. Poblet, *Inorg. Chem.* **2008**, *47*, 7745–7750.
[27] X. Biarnes, A. Ardevol, A. Planas, C. Rovira, A. Laio, M. Parrinello, *J. Am. Chem. Soc.* **2007**, *129*, 10686–10693.
[28] J. Blumberger, B. Ensing, M. L. Klein, *Angew. Chem. Int. Ed.* **2006**, *45*, 2893–2897.
[29] B. Ensing, M. De Vivo, Z. W. Liu, P. Moore, M. L. Klein, *Acc. Chem. Res.* **2006**, *39*, 73–81.
[30] B. Ensing, M. L. Klein, *Proc. Natl. Acad. Sci. USA* **2005**, *102*, 6755–6759.
[31] A. Rodriguez-Fortea, M. Iannuzzi, *J. Phys. Chem. C* **2008**, *112*, 19642–19648.
[32] A. Rodriguez-Fortea, M. Iannuzzi, M. Parrinello, *J. Phys. Chem. B* **2006**, *110*, 3477–3484.
[33] A. Rodriguez-Fortea, M. Iannuzzi, M. Parrinello, *J. Phys. Chem. C* **2007**, *111*, 2251–2258.
[34] A. Stirling, M. Iannuzzi, M. Parrinello, F. Molnar, V. Bernhart, G. A. Luinstra, *Organometallics* **2005**, *24*, 2533–2537.
[35] J. Schemberg, K. Schneider, U. Demmer, E. Warkentin, A. Muller, U. Ermler, *Angew. Chem. Int. Ed.* **2007**, *46*, 2408–2413.
[36] M. T. Pope, A. Muller, *Angew. Chem. Int. Ed. Engl.* **1991**, *30*, 34–48.
[37] ADF 2004.01, Department of Theoretical Chemistry, Vrije Universiteit, Amsterdam.
[38] G. T. te Velde, F. M. Bickelhaupt, E. J. Baerends, C. F. Guerra, S. J. A. Van Gisbergen, J. G. Snijders, T. Ziegler, *J. Comput. Chem.* **2001**, *22*, 931–967.
[39] A. D. Becke, *Phys. Rev. A* **1988**, *38*, 3098–3100.
[40] J. P. Perdew, *Phys. Rev. B* **1986**, *33*, 8822–8824.
[41] S. H. Vosko, L. Wilk, M. Nusair, *Can. J. Phys.* **1980**, *58*, 1200–1211.
[42] J. Andzelm, C. Kolmel, A. Klamt, *J. Chem. Phys.* **1995**, *103*, 9312–9320.
[43] A. Klamt, *J. Phys. Chem.* **1995**, *99*, 2224–2235.
[44] A. Klamt, G. Schuurmann, *J. Chem. Soc. Perkin Trans. 2* **1993**, 799–805.
[45] C. C. Pye, T. Ziegler, *Theor. Chem. Acc.* **1999**, *101*, 396–408.
[46] *CPMD*, IBM Corp., Armonk, NY, **1990**–**2006**; MPI für Festkörperforschung, Stuttgart, **1997**–**2001**.
[47] N. Troullier, J. L. Martins, *Phys. Rev. B* **1991**, *43*, 1993.
[48] S. G. Louie, S. Froyen, M. L. Cohen, *Phys. Rev. B* **1982**, *26*, 1738–1742.
[49] C. Lee, W. Yang, R. Parr, *Phys. Rev. B* **1988**, *37*, 785.
[50] M. Sprik, *J. Chem. Soc. Faraday Trans.* **1998**, *110*, 437.

Received: July 25, 2009
Published Online: October 8, 2009

